Dyes and Pigments 96 (2013) 7–15

Contents lists available at SciVerse ScienceDirect

Dyes and Pigments

journal homepage: www.elsevier.com/locate/dyepig

Analogs of anthocyanins with a 3′,4′-dihydroxy substitution: Synthesis and investigation of their acid–base, hydration, metal binding and hydrogen-donating properties in aqueous solution

Nathalie Mora-Soumille, Sheiraz Al Bittar, Maxence Rosa, Olivier Dangles*

University of Avignon, INRA, UMR408, 84000 Avignon, France

ARTICLE INFO

Article history:
Received 19 May 2012
Received in revised form
3 July 2012
Accepted 9 July 2012
Available online 20 July 2012

Keywords:
Anthocyanin
Flavylium
Glycoside
Synthesis
Aluminum
Antioxidant

ABSTRACT

Glycosides of hydroxylated flavylium ions are proposed as pertinent analogs of anthocyanins, a major class of polyphenolic plant pigments. Anthocyanins with a 3′,4′-dihydroxy substitution on the B-ring (catechol nucleus) are especially important for their metal chelating and electron-donating (antioxidant) capacities. In this work, an efficient chemical synthesis of 3′,4′-dihydroxy-7-*O*-β-D-glucopyranosyloxy-flavylium chloride and its aglycone is reported. Then, the ability of the two pigments to undergo proton transfer (formation of colored quinonoid bases) and add water (formation of a colorless chalcone) is investigated: at equilibrium the colored quinonoid bases (kinetic products) are present in very minor concentrations (<10% of the total pigment concentration) compared to the colorless chalcone (thermodynamic product). The glucopyranosyloxyflavylium ion appears significantly less acidic than the aglycone. The thermodynamics of the overall sequence of flavylium – chalcone conversion is not affected by the β-D-glucosyl moiety while the kinetics appears slower by a factor *ca.* 8. Although the glucopyranosyloxyflavylium ion and its aglycone display similar affinities for Al^{3+}, the Al^{3+}-glucoside complex is more stable than the Al^{3+}-aglycone complex due to the higher sensitivity of the latter to water addition and conversion into the corresponding chalcone. Finally, the glucopyranosyloxyflavylium ion and its aglycone are compared for their ability to reduce the 1,1-diphenyl-2-picrylhydrazyl radical in a mildly acidic water/MeOH (1:1) mixture as a first evaluation of their antioxidant activity. Glycosidation at C_7-OH results in a lower rate constant of first electron transfer to DPPH and a lower stoichiometry (total number of 1,1-diphenyl-2-picrylhydrazyl radicals reduced per pigment molecule).

Anthocyanins are difficult to extract from plants in substantial amount. However, the analogs investigated in this work are of easy access by chemical synthesis and express the physico-chemical properties typical of anthocyanins. They can thus be regarded as valuable models for investigating the coloring, metal-binding and antioxidant properties of these important natural pigments.

1. Introduction

Polyphenols with a 1,2-dihydroxybenzene (catechol) group are common in plants and in our diet. This is for instance the case of caffeic acid (3,4-dihydroxycinnamic acid) and 3′,4′-dihydroxy-flavonoids such as quercetin, (epi)catechin, cyanidin and their derivatives (O-glycosides, esters, oligomers) [1,2]. Those polyphenols are of special interest for their ability to bind metal ions and readily transfer electrons or H-atoms to radicals. As such, they are typically strong in vitro antioxidants. Although the relatively poor bioavailability and extensive metabolism of polyphenols in humans [3] severely restrict the biological significance of in vitro antioxidant tests, it is reasonable to assume that polyphenols with a catechol group may be very important antioxidants in plant and food, and possibly in the digestive tract [4,5].

Anthocyanins are naturally occurring glycosides of flavylium (2-phenyl-1-benzopyrylium) ions substituted by hydroxyl and methoxyl groups [6]. As most polyphenols, they are mainly stored in the mildly acidic aqueous environment of vacuoles within plant cells. Anthocyanins constitute one of the major classes of plant pigments, typically responsible for a wide variety of red to blue colors [7]. One important mechanism of color stabilization and variation is metal – anthocyanin binding, a phenomenon restricted to 3′,4′-dihydroxyflavylium ions. In particular, most blue colors

* Corresponding author. Tel.: +33 490 14 44 46; fax: +33 490 14 44 41.
E-mail address: olivier.dangles@univ-avignon.fr (O. Dangles).

0143-7208/$ – see front matter © 2012 Elsevier Ltd. All rights reserved.
http://dx.doi.org/10.1016/j.dyepig.2012.07.006

found in Nature are complexes of anthocyanins with magnesium, aluminum or iron ions. On the other hand, anthocyanins are also one of the most ubiquitous polyphenol classes in foods, e.g. berries and their products (juices, jams, red wine), red cabbage, red onion and eggplant [2]. As such, anthocyanins may contribute to the protective effects of diets rich in plant products [8]. However, investigating the chemical properties of anthocyanins in line with their activity in plant, food and in humans is somewhat impeded by their difficult extraction and purification from plants and their limited access from commercial sources. Hence glycosides of hydroxylated flavylium ions can be proposed as pertinent anthocyanin analogs. In this work, an efficient chemical synthesis of 3′,4′-dihydroxy-7-*O*-β-D-glucopyranosyloxyflavylium chloride and its aglycone is reported as well as the ability of the two pigments to undergo proton transfer, add water with subsequent conversion into chalcones, bind Al^{3+} and deliver electrons to the DPPH (1,1-diphenyl-2-picrylhydrazyl) radical.

2. Experimental

2.1. Materials and instruments

All starting materials were obtained from commercial suppliers and were used without purification. Purifications were performed by column chromatography on Merck Si60 silica gel (40–63 μm) and by elution on Varian bond elut C18 silica gel cartridges.

^{1}H and ^{13}C NMR spectra were recorded on an Advance DPX300 Bruker apparatus at 300.13 MHz (^{1}H) or 75.46 MHz (^{13}C). Chemical shifts (δ) in ppm relative to tetramethylsilane, ^{1}H–^{1}H coupling constants (J) in Hz. High-resolution mass spectrometry (HRMS) analyses were carried out on Qstar Elite instrument (Applied Biosystems SCIEX). Mass detection was performed in the positive electrospray ionization mode. HPLC analyses were performed on a Waters HPLC system consisting of a 600E pump, a 717 autosampler, a 2996 photodiode array detector, an in-line AF degasser and a Millenium workstation. A LichroCart 250-4 Lichrospher 100 RP18e column (250 × 4.6 mm, 5 μm particle size) was used for chromatographic separations at 25 °C. The solvent system was a gradient of A (5% HCO_2H in MeCN/H_2O 1/1) and B (5% HCO_2H in H_2O) with 10% A at 0 min and 100% A at 60 min (flow rate = 1 mL min^{-1}). UV–Vis absorption spectra were recorded on an Agilent 8453 diode array spectrometer equipped with a magnetically stirred quartz cell (optical path length = 1 cm). The temperature in the cell was controlled by means of a water-thermostated bath at 25 ± 0.1 °C.

2.2. Chemical syntheses

2.2.1. 3,4-Dihydroxyacetophenone

A mixture of activated zinc powder (5 g, 76 mmol), ω-chloro-3,4-dihydroxyacetophenone (5 g, 27 mmol), THF (120 mL) and acetic acid (30 mL) was vigorously stirred for 2 days at room temperature. After filtration and concentration under reduced pressure, EtOAc (100 mL) was added. The organic layer was washed with water (3 × 100 mL), dried over Na_2SO_4 and evaporated. The crude product was purified by column chromatography (SiO_2, cHex/EtOAc, 1:1 v/v) to give compound 3,4-dihydroxyacetophenone as a white amorphous powder (3.7 g). Yield 90%. ^{1}H NMR [$CDCl_3$]: δ = 2.53 (s, 3H, $COCH_3$), 5.99 (1H, s, OH), 6.19 (1H, s, OH), 6.96 (1H, d, J = 8.3, H_5), 7.55 (1H, dd, J = 2.0 and 8.3, H_6), 7.67 (1H, d, J = 2.0, H_2). ^{13}C NMR [$CDCl_3$]: δ = 24.9 (CH_3), 114.4, 114.6 (C_1, C_5), 122.2 (C_2), 129.2 (C_6), 145.0 (C_3), 150.9 (C_4), 198.4 (C=O). HPLC-UV/Vis t_R = 14.2 min, λ_{max} = 276 nm.

2.2.2. 3′,4′,7-Trihydroxyflavylium chloride (**P1**)

A solution of equimolar amounts (4 mmol) of 2,4-dihydroxybenzaldehyde and 3,4-dihydroxyacetophenone in distilled EtOAc (10 mL) was cooled to 0 °C. Gaseous HCl (generated by action of 98% H_2SO_4 on solid NaCl) was gently bubbled through the solution for 90 min. The mixture was kept at 4 °C for 3 days, then filtered. More precipitate was collected after evaporation of the filtrate and addition of diethyl ether (Et_2O). After precipitation in EtOAc, **P1** was obtained as a red powder (0.651 g, yield 56%). The purity of **P1** was carefully checked by reversed-phase HPLC. ^{1}H NMR [0.2 M TFA-d in CD_3OD]: δ = 7.08 (1H, d, J = 8.8, $H_{5'}$), 7.40 (1H, dd, J = 2.2 and 8.8, H_6), 7.46 (1H, d, J = 2.2, H_8), 7.84 (1H, d, J = 2.2, $H_{2'}$), 8.00 (1H, dd, J = 2.2 and 8.8, $H_{6'}$), 8.11 (1H, d, J = 8.8, H_5), 8.24 (1H, d, J = 8.8, H_3), 8.99 (1H, d, J = 8.8, H_4). ^{13}C NMR [0.2 M TFA-d in CD_3OD]: δ = 103.0 (C_8), 112.9 (C_3), 115.7 ($C_{2'}$), 117.3 ($C_{5'}$), 119.0 (C_{10}), 121.0 ($C_{1'}$), 121.5 (C_6), 125.7 ($C_{6'}$), 133.1 (C_5), 147.8 ($C_{3'}$), 153.1 (C_4), 156.7 ($C_{4'}$), 159.4 (C_9), 169.3 (C_7), 173.1 (C_2). HRMS m/z = 255.0652 (M^+, 255.0652 calculated for $C_{15}H_{11}O_4^+$). UV/Vis (0.13 M aqueous HCl): ε(470 nm) = 38,400 M^{-1} cm^{-1}. HPLC-UV/Vis t_R = 24.1 min, λ_{max} = 472 nm.

2.2.3. 4-(2′,3′,4′,6′-Tetra-O-acetyl-β-D-glucopyranosyloxy)-2-hydroxybenzaldehyde

A solution of tetra-*O*-acetyl-α-D-glucopyranosylbromide (9.25 g, 1.5 equiv.) in CH_2Cl_2 (25 mL) was added to a solution of 2,4-dihydroxybenzaldehyde (2.07 g, 15 mmol) and tris(2-(2-methoxyethoxy)ethyl)amine (7.20 mL, 1.5 equiv.) in 1 M $NaHCO_3$/1 M KCl (25 mL, 1/1, v/v). The mixture was refluxed for 48 h. After addition of H_2O (100 mL) and extraction with CH_2Cl_2 (3 × 100 mL), the combined organic phases were successively washed with 1 M HCl (2 × 100 mL) and H_2O (2 × 100 mL), dried over Na_2SO_4 and concentrated. The residue was purified on silica gel (eluent EtOAc/cyclohexane (3/7, v/v)) to afford the target compound as a white powder (5.62 g, yield 80%). ^{1}H NMR [$CDCl_3$]: δ = 2.08 (12H, s, 4 CH_3 of Ac groups), 3.95 (1H, m, $H_{5'}$), 4.17–4.33 (2H, 2dd, J = 12.4 and 5.8, J = 12.4 and 2.3, $H_{6'}$), 5.14–5.32 (4H, m, $H_{1'}$, $H_{2'}$, $H_{3'}$, $H_{4'}$), 6.54 (1H, s, H_3), 6.59 (1H, d, J = 8.5, H_5), 7.47 (1H, d, J = 8.5, H_6). ^{13}C NMR [$CDCl_3$]: δ = 20.6 (4 CH_3 of Ac groups), 61.8 ($C_{6'}$), 68.1 ($C_{4'}$), 70.8 ($C_{2'}$), 72.3 ($C_{5'}$), 72.5 ($C_{3'}$), 97.6 ($C_{1'}$), 103.5 (C_3), 109.6 (C_5), 116.6 (C_6), 135.4 (C_1), 163.1 (C_2), 164.0 (C_4), 169.2–170.6 (4 C=O of Ac groups), 194.9 (CHO).

2.2.4. 3′,4′-Dihydroxy-7-O-β-D-glucopyranosyloxyflavylium chloride (**P2**)

Equimolar amounts (1 mmol) of 3,4-dihydroxyacetophenone and 4-(2′,3′,4′,6′-tetra-O-acetyl-β-D-glucopyranosyloxy)-2-hydroxybenzaldehyde were dissolved in dry EtOAc (10 mL) and cooled to 0 °C. Gaseous HCl was gently bubbled through the solution under stirring during 60 min. The deep-red solution was then allowed to stay at −18 °C for 6 days and filtered. Et_2O was added to the filtrate to ensure complete precipitation. The solid was dissolved in MeOH (20 mL) under Ar and a solution of MeONa in MeOH was added until pH 9 (wet pH paper). After stirring for 1.5 h at room temperature, 1 M HCl was added until pH 1 (wet pH paper). The mixture was kept at 4 °C for 12 h, then concentrated under reduced pressure. The residue was dissolved in 0.01 M HCl (2 mL) and loaded on a C18 cartridge. After elution with 100 mL of 0.01 M HCl to remove contaminating NaCl, **P2** was eluted with 70 mL of 0.2 M HCl in MeOH. After evaporation of solvent under reduced pressure, **P2** was obtained as a red powder (0.34 g, yield 75%). The purity of **P2** was carefully checked by reversed-phase HPLC. ^{1}H NMR [0.2 M TFA-d in CD_3OD]: δ = 3.47 (1H, *t*, J = 9.2, $H_{4''}$), 3.55–3.61 (2H, m, $H_{3''}$, $H_{2''}$), 3.69–3.79 (2H, m, $H_{5''}$, $H_{6''}$), 3.99 (1H, m, $H_{6''}$), 5.37 (1H, d, J = 6.7, $H_{1''}$), 7.11 (1H, d, J = 8.8, $H_{5'}$), 7.63 (1H, dd, J = 2.2 and 8.9, H_6), 7.91 (1H, d, J = 2.2, H_8), 7.95 (1H, d, J = 2.2,

$H_{2'}$), 8.12 (1H, dd, $J = 2.2$ and 8.8, $H_{6'}$), 8.24 (1H, d, $J = 8.9$, H_5), 8.42 (1H, d, $J = 8.9$, H_3), 9.08 (1H, d, $J = 8.9$, H_4). ^{13}C NMR [0.2 M TFA-d in CD_3OD]: $\delta = 62.5$ ($C_{6''}$), 71.2 ($C_{4''}$), 74.6 ($C_{2''}$), 77.8 ($C_{5''}$), 78.7 ($C_{3''}$), 101.9 ($C_{1''}$), 105.0 (C_8), 109.3 (C_3), 115.5 ($C_{2'}$), 116.9 ($C_{5'}$), 118.3 (C_{10}), 121.6 ($C_{1'}$), 122.3 (C_6), 127.5 ($C_{6'}$), 133.0 (C_5), 148.7 ($C_{3'}$), 153.8 (C_4), 158.6 ($C_{4'}$), 159.2 (C_9), 167.0 (C_7), 175.0 (C_2). HRMS $m/z = 417.1178$ (M^+, 417.1180 calculated for $C_{21}H_{21}O_9^+$). UV/Vis (0.13 M aqueous HCl): ε(466 nm) = 14300 M^{-1} cm^{-1}. HPLC-UV/Vis $t_R = 15.3$ min, $\lambda_{max} = 467$ nm.

2.3. Spectroscopic measurements

2.3.1. Proton transfer and hydration reactions

To 2 mL of a 0.05 M acetate buffer (pH 3–6) containing 0.5 M NaCl and placed in the spectrometer cell was added a small volume (20–40 μL) of a concentrated solution of pigment in acidified MeOH (0.2 M HCl). The pigment concentration in the cell was 50 μM. A first UV–visible spectrum was recorded immediately for pK_a determination. A second UV–visible spectrum was recorded after overnight equilibration in the dark for pK'_h determination. For investigating the kinetics of flavylium − chalcone conversion, UV–visible spectra were recorded at regular time intervals (90 s) over 2 h following pigment addition. Each experiment was repeated three times at different pH.

2.3.2. Aluminum complexation

To 2 mL of a 0.1 M acetate buffer (pH 4) placed in the spectrometer cell were successively added 50 μL of Al^{3+} solution (prepared from $Al_2(SO_4)_3$, $18H_2O$, concentration range: 1–10 mM) in 0.05 M aqueous HCl and 50 μL of a freshly prepared 2 mM pigment solution in acidified MeOH (0.1 M HCl). Spectra were typically recorded every 0.5 s over 1 min or every 15 s over 15 min. Spectra were also recorded after overnight equilibration.

2.3.3. Hydrogen abstraction by DPPH

To 1 mL of a freshly prepared 0.2 mM solution of DPPH in MeOH was added 1 mL of 0.1 M acetate buffer (pH 3.5) in the spectrometer cell (final pH *ca.* 4.4). Aliquots (20–60 μL) of a freshly prepared 0.1 mM solution of the antioxidant in acidified MeOH (0.01 M HCl). Spectra were recorded every 0.5 s over 2 min for the determination of rate constants and partial stoichiometries. Kinetic runs over 60 min were used for the determination of total stoichiometries.

2.4. Data analysis

All calculations were carried with the Scientist program (MicroMath, Salt Lake City, USA). Curve-fittings were achieved through least square regression and yielded optimized values for the parameters (rate constants, thermodynamic constants, molar absorption coefficients, stoichiometries, *see eqs in text*). Standard deviations are reported. Good (>0.99) to excellent (>0.999) correlation coefficients were typically obtained.

3. Results and discussion

3.1. Synthesis of pigments

The route for the synthesis of 3′,4′-dihydroxy-7-*O*-β-D-glucopyranosyloxyflavylium chloride (**P2**) was adapted from one of our previous work [9] reporting the synthesis of 3′,7-dihydroxy-4′-*O*-β-D-glucopyranosyloxyflavylium chloride (Scheme 1). Due to the strong hydrogen bond between the carbonyl group and C_2-OH of 2,4-dihydroxybenzaldehyde, the latter group is probably much less acidic than C_4-OH. Consequently, glycosidation under mildly alkaline phase transfer conditions regioselectively took place at C_4-OH. The flavylium chromophore was then constructed via acid-catalyzed aldol condensation followed by cyclization and subsequent dehydration. Methanolysis of the acetate protecting groups, acidification and purification afforded pigment **2** in good yield.

3.2. Structural transformations in water

When the pH is increased from 2 to 6, flavylium ions (AH^+) are typically converted into neutral quinonoid bases (A, kinetic products) by proton transfer (thermodynamic constant K_a) and in a mixture of colorless forms (thermodynamic products) by the following sequence (Scheme 2): water addition at C_2 yielding hemiketal B (thermodynamic constant K_h), cycle-chain tautomerization of B into (*Z*)-chalcone C_Z (thermodynamic constant K_t) and isomerization of C_Z into (*E*)-chalcone C_E (thermodynamic constant K_i) [6,10,11]. Due to their planarity and extensive electron delocalization over the 3 rings, flavylium ions lacking an O-glycosyloxy group at C_3 are less prone to water addition than natural anthocyanins. Consequently, the flavylium ions of **P1** and **P2** are slowly converted into C_E with no significant accumulation of hemiketal B

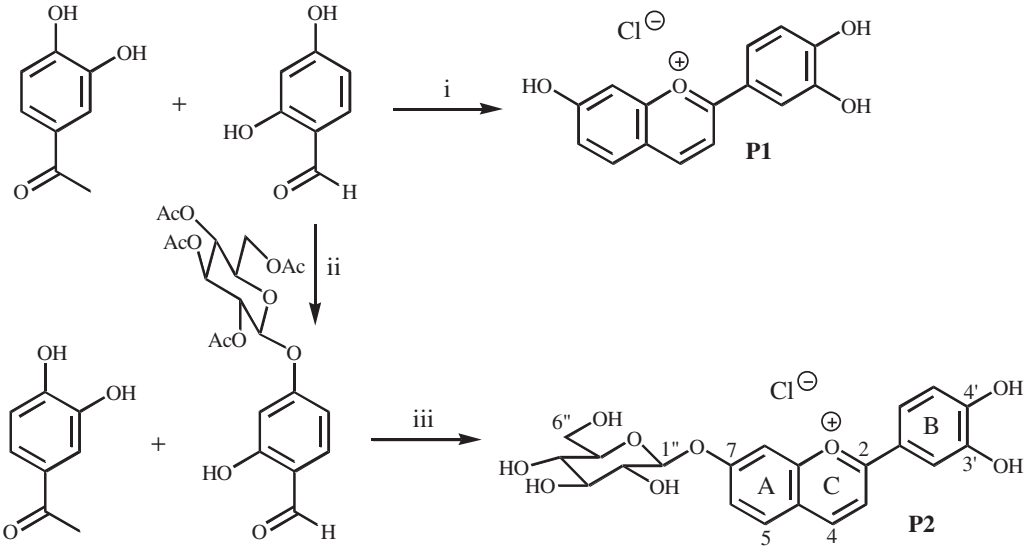

Scheme 1. Chemical synthesis of **P1** and **P2**: (i) Gaseous HCl, AcOEt. (ii) tetra-*O*-acetyl-α-D-glucopyranosylbromide, tris(2-(2-methoxyethoxy)ethyl)amine in CH_2Cl_2/H_2O (1 M $NaHCO_3$, 1 M KCl). (iii) Gaseous HCl, AcOEt, then MeONa, MeOH, then aq. HCl.

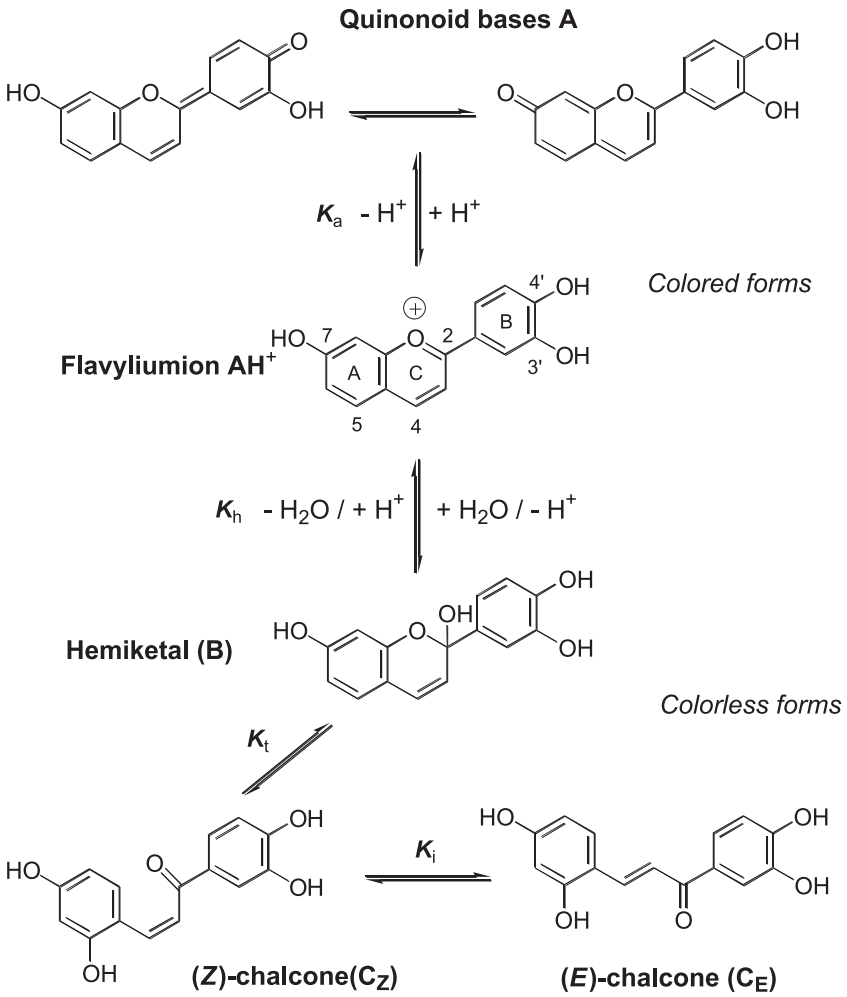

Scheme 2. Structural transformations of 3′,4′,7-trihydroxyflavylium ion (**P1**) in mildly acidic aqueous solution.

and C_Z. This particular behavior makes it possible to independently investigate proton transfer and chalcone formation. Thus, addition of a strongly acidic concentrated solution of **P1** or **P2** in MeOH to aqueous buffers at pH 3–6 with immediate recording of the UV–visible spectra permits the determination of the thermodynamic constant of proton transfer ($K_a = [H^+][A]/[AH^+]$) while the UV–visible spectra recorded after overnight equilibration give access to the overall thermodynamic constant of water addition ($K'_h = K_h K_t K_i = [H^+][C_E]/[AH^+]$). The typical UV–visible spectra of AH^+, A and C_E are shown in Fig. 1.

Combining the Beer's law, the expressions of the thermodynamic constants K_a and K'_h and the equation of pigment conservation readily permits the derivation of the changes in visible absorbance as a function of pH for freshly prepared pigment solution (eq. (1), water addition neglected) and solutions equilibrated overnight (eq. (2)).

$$A_0 = A_{AH}\frac{1 + r_A K_a 10^{pH}}{1 + K_a 10^{pH}} \tag{1}$$

$$A_f = A_{AH}\frac{1 + r_A K_a 10^{pH}}{1 + (K_a + K'_h)10^{pH}} \tag{2}$$

$A_{AH} = \varepsilon_{AH} C$ (absorbance of a strongly acidic pigment solution containing the sole flavylium ion, C: total pigment concentration), $r_A = \varepsilon_A/\varepsilon_{AH}$ (ratio of the molar absorption coefficients of quinonoid bases and flavylium ion).

Eqs. (1) and (2) were used in the curve-fitting analyses for pK_a and pK'_h determination, respectively (Fig. 2, Table 1). Combining eqs. (1) and (2) gives eq. (3), which can also be used for the estimation of K'_h from the amplitude $\Delta A = A_0 - A_f$ of the time-dependence of the visible absorbance during water addition (Fig. 3, Table 2).

$$K'_h = \left(10^{-pH} + K_a\right)\frac{A_0 - A_f}{A_f} = \left(10^{-pH} + K_a\right)\frac{\Delta A}{A_0 - \Delta A} \tag{3}$$

Unexpectedly, with both **P1** and **P2**, when the observed rate constant of flavylium hydration k_h^{obs} is plotted as a function of the proton concentration, a monotonous increase is observed (Fig. 4), which is in sharp contrast with the usual behavior [6]. Indeed, quinonoid bases are less electrophilic than the flavylium ion and do not undergo water addition in mildly acidic solution. Hence, k_h^{obs} normally decays when the pH increases as a consequence of less flavylium ion and more quinonoid bases being present in solution. One has: $k_h^{obs} = k'_h x_{AH} + k'_{-h}[H^+]$ (k'_h: overall rate constant for the flavylium to chalcone conversion, k'_{-h}: overall rate constant for the chalcone to flavylium conversion) with $x_{AH} + x_A = 1$, $K_a = [H^+]x_A/x_{AH}$. Combining these equations yields eq. (4).

$$k_h^{obs} = \frac{k'_h}{1 + \dfrac{K_a}{[H^+]}} + k'_{-h}[H^+] \tag{4}$$

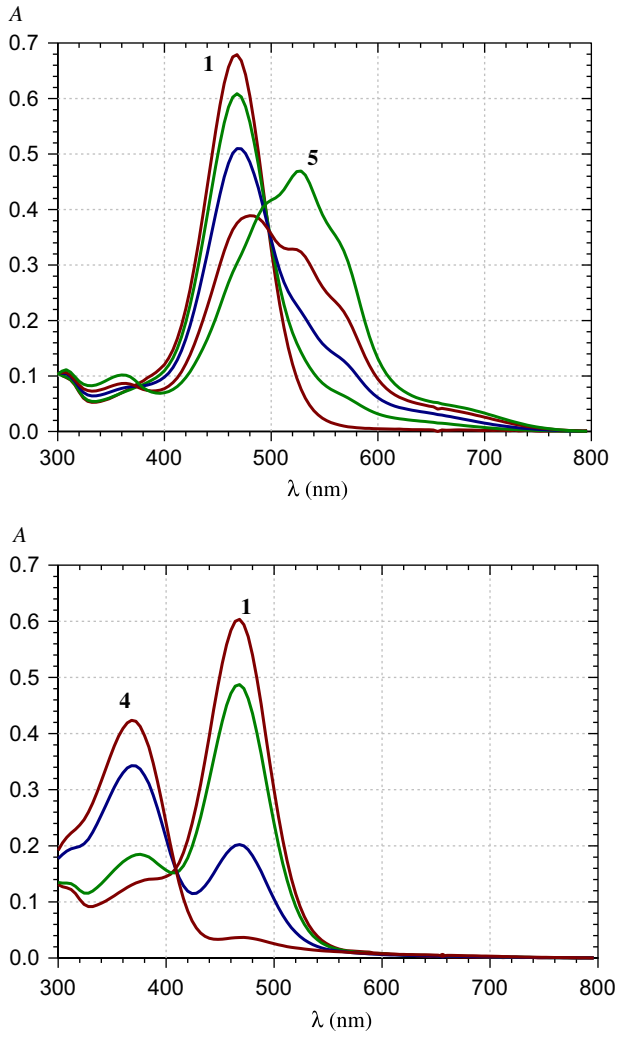

Fig. 1. pH-dependence of the UV–visible spectra of **P2**. *Top*: Spectral measurements immediately after addition of pigment to buffer (**1**: pH 2.0, **2**: pH 4.0, **3**: pH 4.4, **4**: pH 5.0, **5**: pH 6.0). *Down*: Spectral measurements on solutions equilibrated overnight (**1**: pH 2.0, **2**: pH 3.0, **3**: pH 3.5, **4**: pH 4.0).

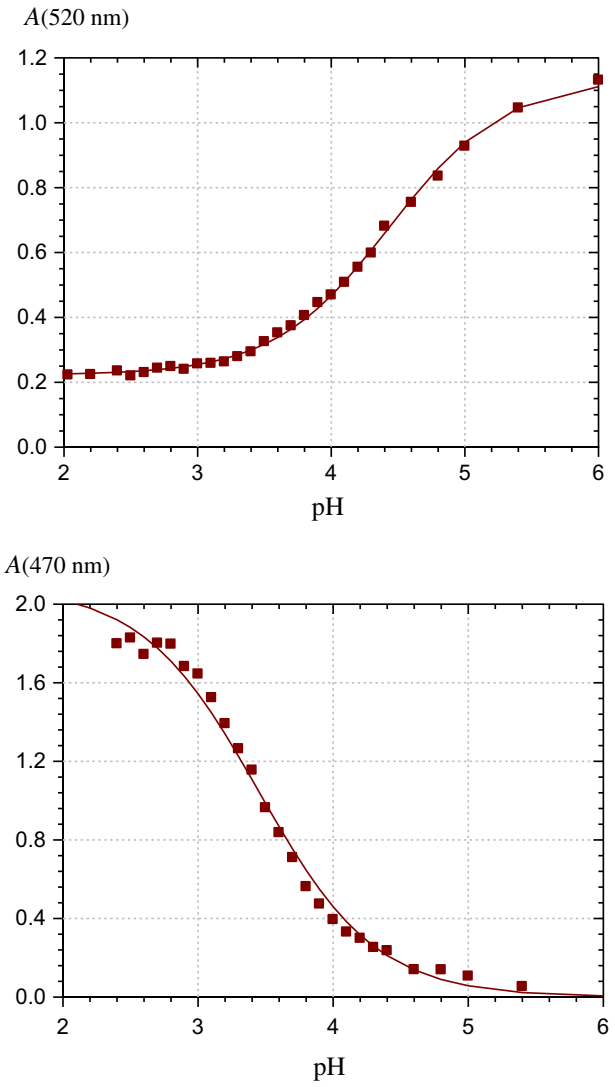

Fig. 2. pH dependence of the visible absorbance of **P1**. *Top*: Spectral measurements immediately after addition of pigment to buffer (the solid line is the result of the curve-fitting according to eq. (1)). *Down*: Spectral measurements on solutions equilibrated overnight the solid line is the result of the curve-fitting according to eq. (2).

Obviously, eq. (4) does not hold with **P1** and **P2**. Unlike natural anthocyanins, those flavylium ions are strongly conjugated as no substituent at C_3 restricts the planarity of the 3 rings. Hence, conjugation of $O_{4'}$ and O_7 with the pyrylium C-ring must be very strong and this may lower the positive charge at C_2 to the point that hydration only takes place via the minor hydroxide ion. If so, the observed rate constant of flavylium hydration can be rewritten as: $k_h^{obs} = k'_h x_{AH}[HO^-] + k'_{-h}$. Consequently, eq. (4) is changed into eq. (5) (K_w: ionic product of water):

$$k_h^{obs} = \frac{k'_h K_w}{[H^+] + K_a} + k'_{-h} \quad (5)$$

Eq. (5) actually permits a good curve-fitting of k_h^{obs} *vs.* proton concentration curve (Fig. 4).

With $K_a << K'_h$ for both pigments, it can be concluded that the quinonoid bases (kinetic products) are present in very minor concentrations at equilibrium (<10% of the total pigment concentration) compared to the chalcone (thermodynamic product) (Fig. 5). **P2** appears significantly less acidic than **P1** as a consequence of the replacement of the acidic proton at C_7-OH by the β-D-glucosyl moiety. Unexpectedly, **P2** turned out to be rather unstable in mildly acidic conditions (pH > 4–5), thereby complicating the determination of pK'_h from fully equilibrated solutions. This instability may reflect its sensitivity to autoxidation (initiated by unidentified metal traces). The close pK'_h values deduced from the amplitude of the time-dependence of the visible absorbance during water addition (Table 2) show that the thermodynamics of the overall hydration-ring opening-(*Z*,*E*) isomerization process is not affected by the β-D-

Table 1
Thermodynamic constants of water addition and proton transfer.

Pigment	pK_{obs}	A_{AH}, $r_A = \varepsilon_A/\varepsilon_{AH}$	λ (nm), r (number of points)
P1[a]	4.44(±0.01)	0.22(±0.01), 5.1(±0.1)	520, 0.9992 (28)
P1[b]	3.45(±0.03)	2.09(±0.04), 0	470, 0.996 (25)
P2[a]	4.72(±0.02)	0.085(±0.002), 5.64(±0.15)	526, 0.998 (26)
P2[b]	n.a.[c]	–	–

[a] Spectral measurements immediately after addition of pigment to buffer: $K_{obs} = K_a$. Curve-fitting according to eq. (1).
[b] Spectral measurements on solutions equilibrated overnight: $K_{obs} = K'_h + K_a \approx K'_h$. Curve-fitting according to eq. (2).
[c] Not applicable because of insufficient chemical stability (see section 3.2).

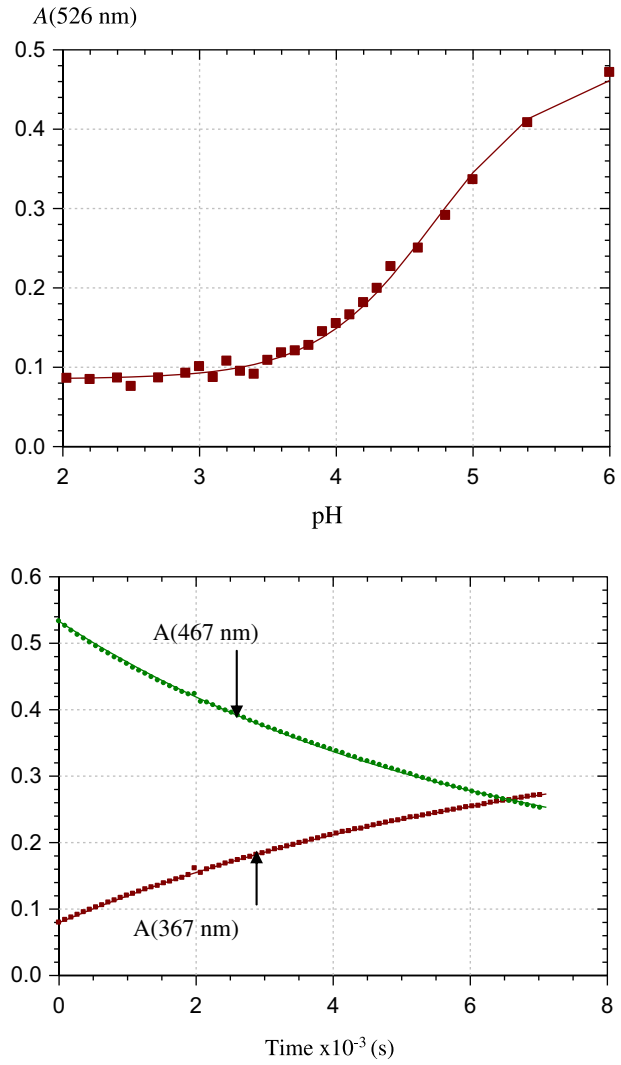

Fig. 3. *Top*: pH-dependence of the visible absorbance of **P2**. Spectral measurements immediately after addition of pigment to buffer (the solid line is the result of the curve-fitting according to eq. (1)). *Down*: Time-dependence of the UV–visible absorbance of **P2** at pH 4.0 (the solid lines are the result of exponential curve-fittings).

glucosyl moiety. Surprisingly, this is not so with the corresponding kinetics. Indeed, at pH 4.0, glycosidation at C_7-OH lowers the rate constant of flavylium consumption by a factor *ca.* 8 (Table 2). As the observed kinetics is governed by the step of chalcone (*Z*,*E*) isomerization, it may be suggested that the +M effect of O_7 weakens the C_3=C_4 double bond by enhancing the conjugation with C_4=O and that this effect is strongly decreased by glycosidation of O_7, thereby making the chalcone (*Z*,*E*) isomerization much slower for **P2** than for **P1** with no impact on the thermodynamics of the reaction.

Table 2
Kinetics of flavylium – chalcone conversion at pH 4.0.

Pigment	$10^5 k_h^{obs}$ (s^{-1})	A_0, ΔA	pK'_h [a]	λ (nm), *r*
P1	121.3(±0.1)	1.70, 1.28	3.38	470, 0.99999
	134.1(±0.3)	0.225, 0.693		377, 0.99995
P2	16.5(±0.2)	0.533, 0.405	3.42	467, 0.9998
	15.7(±0.2)	0.072, 0.295		367, 0.9998

[a] Calculated according to eq. (3).

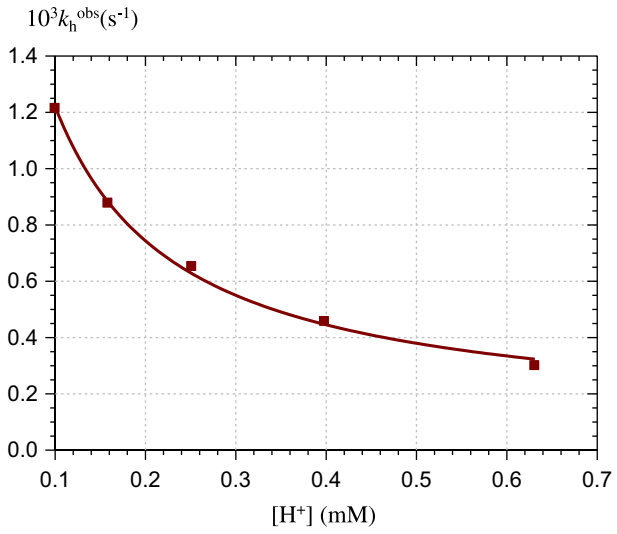

Fig. 4. Dependence of the apparent rate constant of flavylium **P1** hydration as a function of the proton concentration. The solid line is the result of the curve-fitting according to eq. (5): $k'_h = 15.4(\pm0.4) \times 10^6\ M^{-1}\ s^{-1}$, $k'_{-h} = 9.3(\pm2.0) \times 10^{-5}\ s^{-1}$ ($r = 0.999$).

3.3. Aluminum complexation

Anthocyanins having a 1,2-dihydroxy substitution in their B-ring can bind hard metal ions such as Al^{3+} and Fe^{3+} with concomitant removal of the phenolic protons [7,12]. The corresponding chelates display a quinonoid structure that is much more stable than in the absence of metal ions. Consequently, metal binding is a powerful mechanism of color variation and stabilization in plants. In this work, **P1** and **P2** were compared for their ability to bind Al^{3+} in mildly acidic aqueous solutions mimicking their natural medium (vacuoles of plant cells).

When **P1** and **P2** are added to a Al^{3+} solution in a pH 4 acetate buffer, a relatively fast binding of the colored form is observed which is manifested by a decay of the visible absorption band at *ca.* 470 nm (free ligand *L*, a mixture of flavylium and quinonoid bases) and a building-up of a broader absorption band at *ca.* 525 nm characteristic of the metal complex (*ML*) (Fig. 6). Interestingly, the Al^{3+} complex of **P1** appeared much less stable than the one of **P2** as judged from the subsequent decay of *A*(525 nm) and concomitant increase of the absorbance at 370–380 nm featuring free chalcone accumulation (Fig. 7). However, after overnight equilibrium, accumulation of free chalcone was observed with both **P1** and **P2** although in much lower concentration with the glucoside (Fig. 6). The absorbance–time curves for free ligand consumption and complex and chalcone formation could be analyzed simultaneously according to a simplified mechanism assuming irreversible metal binding (rate constant k_M) and water addition on both the free ligand and its complex (respective rate constants k_h^{obs} and k_h^M). In addition to the Beer's law for the different pigment species (*L*, *ML*, *C*), eqs. (6)–(9) were used in the curve-fittings:

$$-d[L]/dt = k_M[M][L] + k_h^{obs}[L] \quad (6)$$

$$-d[M]/dt = k_M[M][L] - k_h^M[ML] \quad (7)$$

$$d[ML]/dt = k_M[M][L] - k_h^M[ML] \quad (8)$$

$$d[C]/dt = k_h^{obs}[L] + k_h^M[ML] \quad (9)$$

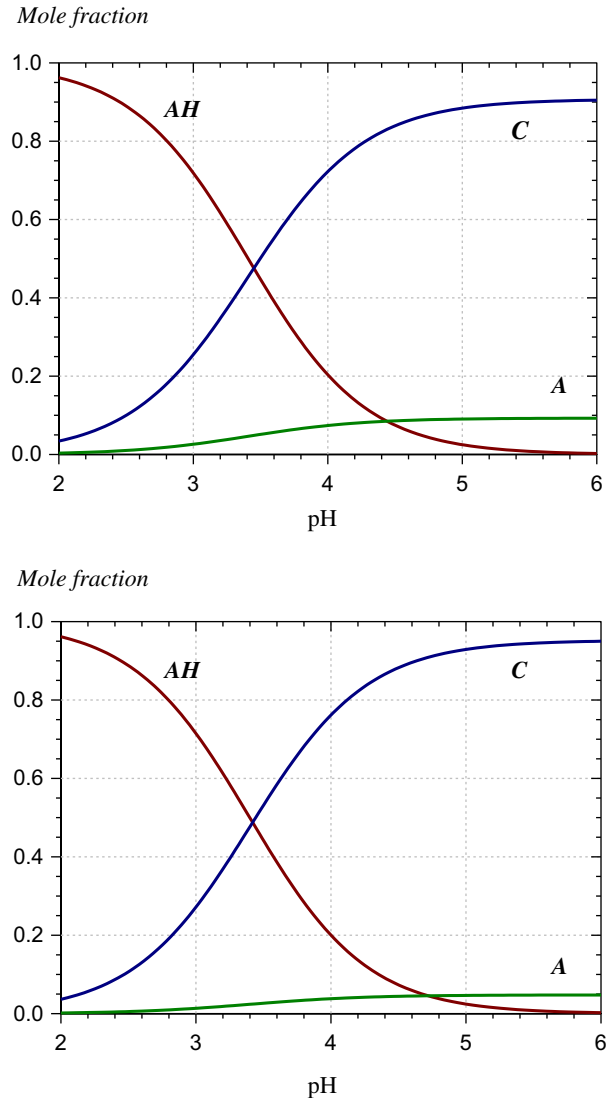

Fig. 5. Speciation diagrams of **P1** (*Top*) and **P2** (*Down*) at equilibrium.

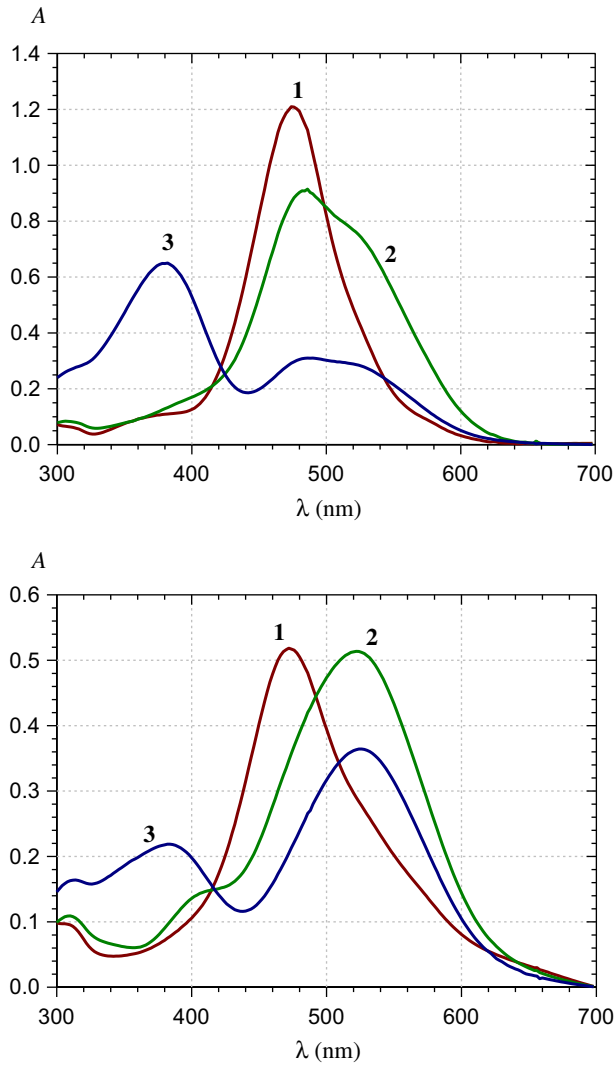

Fig. 6. UV–visible spectra of **P1** (*Top*) and **P2** (*Down*) in the presence of Al^{3+} (4 equiv.) at pH 4. **1**: free ligand, **2**: time of maximal Al^{3+} complexation, **3**: after equilibration overnight.

The optimized values of the observed rate constants are collected in Table 3. It is noteworthy that no satisfactory curve-fitting could be achieved without the hypothesis of water addition onto the complex. In particular, the slow decay of the absorption band of the Al^{3+} – **P1** complex could not be accounted for by assuming reversible metal binding and water addition on the free ligand only. From this kinetic analysis, it is also clear that Al^{3+} binding is faster with **P1** than with **P2** but that the Al^{3+} – **P1** complex is much more prone to water addition than the Al^{3+} – **P2** complex. From this viewpoint, glycosidation at C_7-OH can be regarded as an efficient way to increase the stability of the Al^{3+} complex in mildly acidic aqueous solution. Surprisingly, the values of the observed rate constant for free flavylium hydration (k_h^{obs}) are higher than those estimated in the absence of Al^{3+} (Table 2), especially for **P2**. It is unclear why the free flavylium – chalcone conversion is faster in the presence of Al^{3+}. It can however be noted that C_E itself probably binds Al^{3+} as evidenced by the weak bathochomic shift (*ca.* 10 nm) observed when comparing Fig. 1 (lower part, free C_E) and Fig. 6 (lower part). As the kinetics of the overall flavylium – chalcone conversion is governed by the slow step of (*Z*)-(*E*) chalcone isomerization, it can be suggested that Al^{3+} – chalcone binding accelerates the latter step.

The maximal absorbance amplitude at 525 nm (ΔA) was also plotted as a function of the total metal concentration (M_t) and the corresponding curve analyzed by assuming pure 1:1 binding and negligible chalcone formation (eqs. (10) and (11), K_M: metal – pigment binding constant, L_t: total ligand concentration, $\Delta\varepsilon = \varepsilon_{ML}^{525} - \varepsilon_L^{525}$).

$$\Delta A = \Delta\varepsilon(M_t - [M]) \tag{10}$$

$$M_t = [M]\left(1 + \frac{K_M L_t}{1 + K_M[M]}\right) \tag{11}$$

The following K_M values were thus obtained: for **P1**, $K_M = 8.9(\pm 1.3) \times 10^3\ M^{-1}$ ($r = 0.997$), for **P2**, $K_M = 19(\pm 8) \times 10^3\ M^{-1}$ ($r = 0.98$).

Alternatively, for **P2**, the observed first-order rate constant of metal binding (k_M^{obs}) was found to vary linearly with the total metal concentration (Fig. 8, $r = 0.998$). From $k_M^{obs} = k_M M_t + k_{-M}$, estimates for the rate constants of complex formation and dissociation were obtained: $k_M = 44(\pm 2)\ M^{-1}\ s^{-1}$, $k_{-M} = 20(\pm 4) \times 10^{-4}\ s^{-1}$, from which one deduces: $K_M = k_M/k_{-M} = 22 \times 10^3\ M^{-1}$.

Finally, for **P1**, the overall first-order rate constant of flavylium – chalcone conversion was plotted as a function of M_t and the

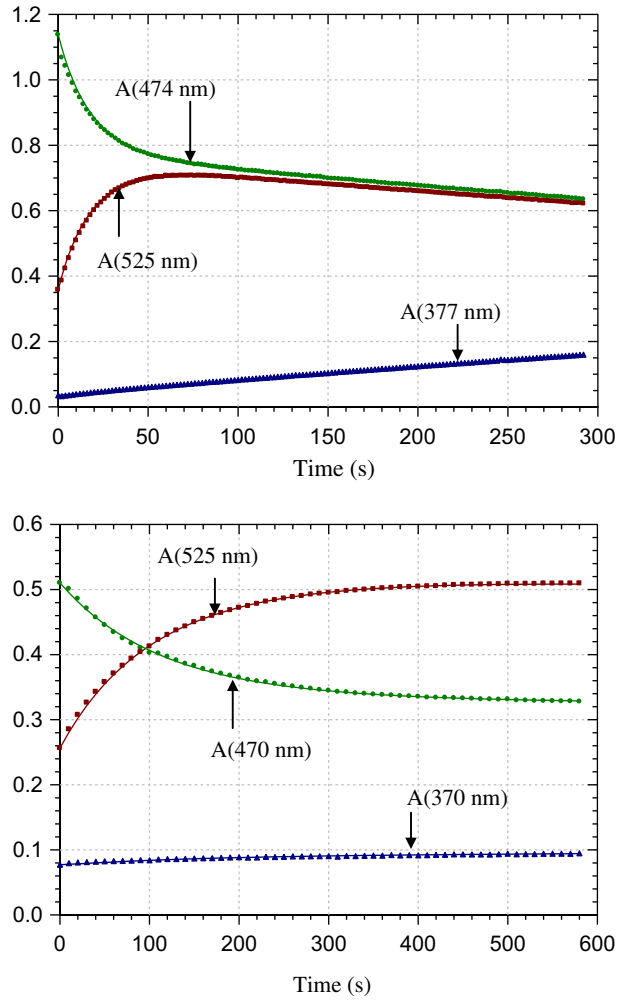

Fig. 7. Time-dependence of the UV–visible absorbance of **P1** (*Top*) and **P2** (*Down*) after addition of Al^{3+} (4 equiv.) at pH 4.0. The solid lines are the result of the curve-fittings according to eqs. (6)–(9).

corresponding curve analyzed according to eqs. (11) and (12) (Fig. 9, $r = 0.996$).

$$k_h^{overall} = \frac{k_h^{obs} + k_h^{M} K_M [M]}{1 + K_M [M]} \qquad (12)$$

Table 3
Kinetic analysis of Al^{3+} binding and water addition at pH 4.0[a].

Pigment	Al^{3+} (equiv.)	k_M (M^{-1} s^{-1})	$10^5 k_h^{obs}$, $10^5 k_h^{M}$ (s^{-1})	ε_{ML}[b] (ε_C[c]) (M^{-1} cm^{-1})
P1	2	486(±3)	302(±7), 82(±1)	19990, 27980 (21920)
	4	288(±1)	324(±6), 64(±1)	21290, 21850 (20480)
	6	257(±2)	341(±14), 54(±1)	24690, 20550 (21960)
	8	195(±1)	614(±23), 38(±1)	23000, 17400 (19950)
	10	161(±1)	467(±26), 29(±1)	27550, 18840 (22390)
P2	2	23.2(±1.0)	284(±9), 6.3(±0.2)	25520, 20600 (4340)
	4	37.3(±1.3)	226(±22), 3.2(±0.3)	16240, 10420 (8140)
	6	41.3(±1.4)	284(±36), 2.5(±0.2)	16550, 9200 (10440)
	8	40.3(±1.1)	315(±36), 1.8(±0.2)	16430, 8970 (11990)
	10	12.6(±0.1)	182(±6), 3.7(±0.1)	15890, 10020 (9250)

[a] **P1**: simultaneous curve-fitting of the absorbance curves at 525, 474 and 377 nm ($\Delta t = 2$ s, $t_f = 5$ min) according to eqs. (6)–(9). **P2**: simultaneous curve-fitting of the absorbance curves at 525, 470 and 370 nm ($\Delta t = 10$ s, $t_f = 15$ min).
[b] First value at 525 nm, second value at 474 nm (**P1**) or 470 nm (**P2**).
[c] At 377 nm (**P1**) or 370 nm (**P2**).

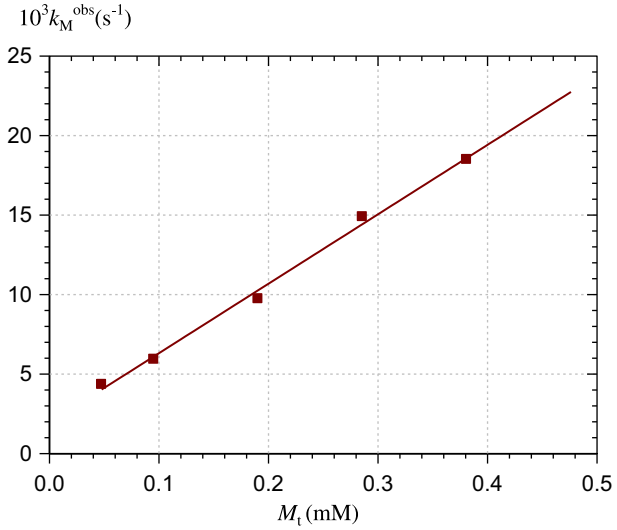

Fig. 8. Plot of the apparent first-order rate constant of Al^{3+} – **P2** binding as a function of the total metal concentration (pH 4.0).

Thus, one obtains estimates for the binding constant as well as for the rate constants of chalcone formation from the free flavylium and its complex: $k_h^{obs} = 195(\pm 12) \times 10^{-5}$ s^{-1}, $k_h^{M} = 45(\pm 1) \times 10^{-5}$ s^{-1}, $K_M = 9.8(\pm 3.5) \times 10^3$ M^{-1}.

In summary, **P1** and **P2** display similar affinities for Al^{3+} ($K_M = 1–2 \times 10^4$ M^{-1}) but the complex of **P2** is more stable as its conversion into the corresponding chalcone is slower.

3.4. Scavenging of the DPPH radical

Polyphenols with a catechol group are potent electron or H-atom donors to radicals due to the relatively stability of the semiquinone radicals thus formed (a combination of electronic and intramolecular hydrogen bonding effects). Semiquinone radicals derived from polyphenols are however rapidly converted into *o*-quinones by disproportionation or scavenging of a second radical. From these reactive intermediates, different pathways (oligomerization, solvent addition, ring cleavage) typically ensue, ultimately

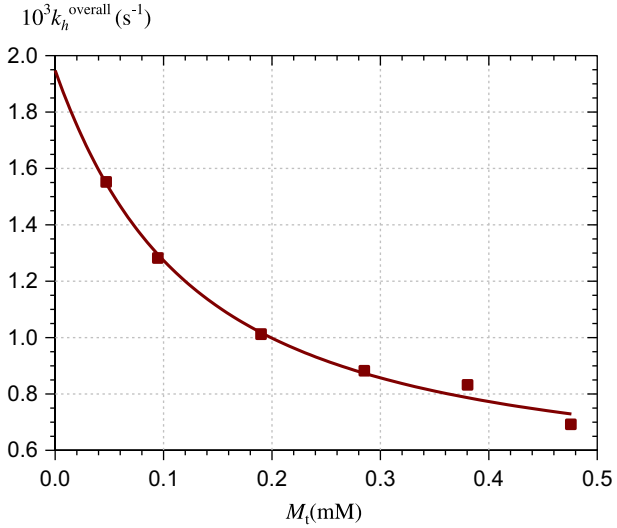

Fig. 9. Plot of the apparent first-order rate constant of flavylium – chalcone conversion for **P1** as a function of the total metal concentration (pH 4.0). The solid line is the result of the curve-fitting according to eq. (12).

giving a complex set of oxidation products [4]. Such reactions may take place in plants where polyphenols act as electron donors for the enzymatic reduction of hydrogen peroxide in vacuoles but also in food and in the digestive tract where polyphenols may protect polyunsaturated lipids from oxidation and/or regenerate the potent phenolic antioxidant α-tocopherol (vitamin E) by H-atom or electron transfer to its aryloxyl radical. Whether in plants, food or the digestive tract, anthocyanins typically experience a mildly acidic aqueous environment. Hence, investigating their electron-donating capacity toward the stable radical DPPH (1,1-diphenyl-2-picrylhydrazyl) in a MeOH/pH 3.5 acetate buffer (1:1) mixture (final pH *ca*. 4.4) is a first acceptable approach to assess their antioxidant activity.

When the pigment is added to the DPPH solution, a fast decrease of the DPPH visible absorption band is observed featuring the transfer of the labile H-atoms of the catechol OH groups. Then, a slower decay follows that reflects the residual H-donating activity of some oxidation products. From the total absorbance amplitude over 1 h ($\Delta A^{515} = A^{515}(t = 1\text{ h}) - A^{515}(t = 0$, i.e. before pigment addition)), the total number of DPPH radicals reduced to the corresponding hydrazine per pigment molecule (total stoichiometry n_{tot}) can be deduced from the following relationship: $n_{tot} = \Delta A^{515}/(\varepsilon^{515}_{DPPH}[\text{pigment}]_0)$ (Table 4) with $\varepsilon^{515}_{DPPH} = 11240\ M^{-1}\ cm^{-1}$ [13].

The fast step was kinetically analyzed according to a model developed in details in our previous work [13,14] and permitting the estimation of the rate constant of first H-atom transfer (k_1) and the partial stoichiometry n (number of DPPH radicals reduced per pigment molecule during the fast step) (Table 4). It is noteworthy that the kinetic analysis had to be conducted at 600 nm so as to avoid interference with the visible absorption of the pigment at the onset of the reaction.

As the catechol group is the critical determinant of the H-donating activity of polyphenols, it may be anticipated that **P2** be as good at scavenging the DPPH radical as **P1**. Surprisingly, this is not so. Not only does **P1** transfer a first H-atom to DPPH *ca*. 4 times as rapidly as **P2**, but also the total number of DPPH radicals reduced by **P1** is *ca*. 3 times as high as by **P2**. As DPPH is a rather bulky radical, part of the lower reactivity of **P2** could be attributed to the steric hindrance brought about by the glucose moiety. It is also important to keep in mind that **P2** is less acidic than **P1**. As the flavylium ion (because of its positive charge) is expected to be a poor electron or H-atom donor and as the kinetic of flavylium − chalcone conversion is much slower than the DPPH-scavenging reaction, rate constant k_1 must essentially reflect the ability of the quinonoid bases to transfer an H-atom to DPPH. Moreover, **P1** can form both $A_{4'}$ and A_7 tautomers whereas $A_{4'}$ is the only possible quinonoid base for **P2**. Overall, it could be suggested that A_7 makes a major contribution to the radical-scavenging activity of **P1** via H-transfer from $C_{4'}$-OH. Alternatively, the anionic quinonoid base $A_{4',7}$, although in minor concentration, could be the true electron-donor due to the extended electron-delocalization on the chromophore. Indeed, upon deprotonation, $A_{4'}$ and A_7 merge into a single π-electron-rich anion with a concomitant spectacular rise of the HOMO by *ca*. 4 eV (HyperChem software, AM1 parametrization).

On the other hand, the total stoichiometry value is defined by the fate of the antioxidant during oxidative degradation. In a previous work [15], we showed that upon two-electron oxidation **P1** forms an *o*-quinone that undergoes water addition on the C- and A-rings. The quinonoid bases thus formed display an additional OH groups and must also participate in radical-scavenging, thereby prolonging the activity. It is possible that glycosidation at C_7-OH somehow hinders these sequences of oxidation/water addition, thus resulting in lower n_{tot} values.

Table 4
DPPH scavenging by **P1** and **P2** in MeOH/pH 3.5 acetate buffer (1:1).

Pigment, conc. (μM)	DPPH conc. (μM)	k_1 ($M^{-1}\ s^{-1}$)[a]	n[a]
P1, 10	77.0	4305(±64)	2.22(±0.01)
P1, 15	83.8	4290(±160)	2.09(±0.03)
P1, 15	77.4	5354(±70)	2.67(±0.01)
P2, 15	64.6	1426(±37)	0.85(±0.01)
P2, 15	64.8	1355(±48)	0.70(±0.01)
P2, 25	70.8	1368(±32)	0.91(±0.01)
P2, 25	66.5	1363(±11)	0.93(±0.01)
P2, 30	65.9	1066(±10)	0.82(±0.01)

From the absorbance amplitude at 515 nm over 1 h: total number of DPPH radicals reduced per pigment molecule n_{tot} = 4.0(±0.2) for **P1**, 1.38(±0.04) for **P2** (means from triplicates).

[a] Curve-fitting of A^{600} *vs*. time curves (see model in text) over the 40 first seconds following pigment addition: k_1: rate constant of first H-atom abstraction, n: number of DPPH radicals reduced per pigment molecule.

4. Conclusion

3′,4′-Dihydroxy-7-*O*-β-D-glucopyranosyloxyflavylium chloride (**P2**), which has been synthesized in this work at a scale of several hundreds of mg, is a valuable model of natural anthocyanins. Its glucose moiety improves the water solubility while only moderately affecting the acid–base and hydration properties of the chromophore. Due to its catechol group, **P2** can be used to investigate the affinity of anthocyanins for metal ions and their ability to deliver electrons to radicals, two characteristics that have a strong impact on the pigmentation and nutritional properties of anthocyanins.

References

[1] Quideau S, Deffieux D, Douat-Casassus C, Pouysegu L. Plant polyphenols: chemical properties, biological activities, and synthesis. Angew Chem Int Ed 2011;50:586–621.

[2] Perez-Jimenez J, Neveu V, Vos F, Scalbert A. Systematic analysis of the content of 502 polyphenols in 452 foods and beverages: an application of the phenol-explorer database. J Agric Food Chem 2010;58:4959–69.

[3] Crozier A, Jaganath IB, Clifford MN. Dietary phenolics: chemistry, bioavailability and effects on health. Nat Prod Rep 2009;26:1001–43.

[4] Dangles O. Antioxidant activity of plant phenols: chemical mechanisms and biological significance. Curr Org Chem 2012;16:692–714.

[5] Frankel EN, Finley JW. How to standardize the multiplicity of methods to evaluate natural antioxidants. J Agric Food Chem 2008;56:4901–8.

[6] Pina F, Melo MJ, Laia CAT, Parola AJ, Lima JC. Chemistry and applications of flavylium compounds: a handful of colours. Chem Soc Rev 2012;41:869–908.

[7] Yoshida K, Mori M, Kondo T. Blue flower color development by anthocyanins: from chemical structure to cell physiology. Nat Prod Rep 2009;26:857–964.

[8] Tsuda T. Dietary anthocyanin-rich plants: biochemical basis and recent progress in health benefits studies. Mol Nutr Food Res 2012;56:159–70.

[9] El Hajji H, Dangles O, Figueiredo P, Brouillard R. 3′-(β-D-Glycopyranosyloxy) flavylium ions: synthesis and investigation of their properties in aqueous solution. Hydrogen bonding as a mean of colour variation. Helv Chim Acta 1997;80:398–413.

[10] Dangles O, Saito N, Brouillard R. Kinetic and thermodynamic control of flavylium hydration in the pelargonidin–cinnamic acid complexation. Origin of the extraordinary flower color diversity of *Pharbitis nil*. J Am Chem Soc 1993; 115:3125–32.

[11] Nave F, Petrov V, Pina F, Teixeira N, Mateus N, de Freitas V. Thermodynamic and kinetic properties of a red wine pigment: catechin-(4,8)-malvidin-3-*O*-glucoside. J Phys Chem B 2010;114:13487–96.

[12] Dangles O, Elhabiri M, Brouillard R. Kinetic and thermodynamic investigation of the aluminium–anthocyanin complexation in aqueous solution. J Chem Soc Perkin Trans 1994;2:2587–96.

[13] Goupy P, Loonis M, Dufour C, Dangles O. A quantitative kinetic analysis of hydrogen transfer reactions from dietary polyphenols to the DPPH radical. J Agric Food Chem 2003;51:615–22.

[14] Goupy P, Bautista-Ortin AB, Fulcrand H, Dangles O. Antioxidant activity of wine pigments derived from anthocyanins: hydrogen transfer reactions to the DPPH radical and inhibition of the heme-induced peroxidation of linoleic acid. J Agric Food Chem 2009;57:5762–70.

[15] Dangles O, Fargeix G, Dufour C. Antioxidant properties of anthocyanins and tannins: a mechanistic investigation with catechin and the 3′,4′,7-trihydroxyflavylium ion. J Chem Soc Perkin Trans 2000;2:1653–63.